Langmuir

Article

pubs.acs.org/Langmuir

Facile Synthesis of AuPt Alloy Nanoparticles in Polyelectrolyte Multilayers with Enhanced Catalytic Activity for Reduction of 4-Nitrophenol

Chengcan Chu and Zhaohui Su*

State Key Laboratory of Polymer Physics and Chemistry, Changchun Institute of Applied Chemistry, Chinese Academy of Sciences, 5625 Renmin Street, Changchun 130022, P. R. China

Supporting Information

ABSTRACT: In this work, bimetallic AuPt alloy nanoparticles were synthesized *in situ* in polyelectrolyte multilayers (PEMs) via an ion-exchange and coreduction process, in which the PEM support also served to suppress the Au−Pt phase separation, and thus enabled formation of AuPt alloy nanoparticles over a wide composition range. The PEM supported AuPt alloy nanoparticles exhibited higher catalytic activity than Au and Pt monometallic ones for the reduction of 4-nitrophenol by $NaBH_4$, showing synergistic effects between Au and Pt. This work provides a facile approach to *in situ* synthesis of polymer supported bimetallic nanoparticles of tailored composition for optimum performance in catalysis and other applications.

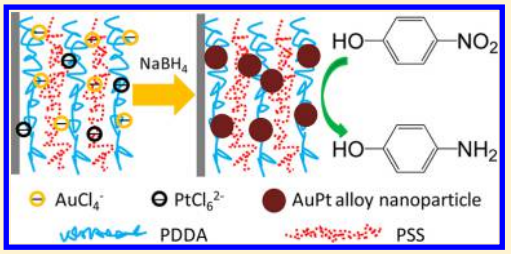

INTRODUCTION

In recent years, bimetallic nanoparticles have attracted significant attention due to their fascinating optical, electronic, and catalytic properties as compared to their monometallic counterparts, and their application in catalysis, sensors, and surface-enhanced Raman scattering among others has been an area of intense research.[1−3] Among the various bimetallic nanoparticles reported, AuPt alloy nanoparticles are of particular interest in catalysis. For example, Ebitani et al. found that hydrotalcite-supported AuPt alloy nanoparticles exhibit higher selectivity than the monometallic ones for the oxidation of the primary hydroxyl group in glycerol and 1,2-propanediol,[4] and Shukla et al. reported that carbon-supported AuPt alloy nanoparticles are a superior cathode catalyst than Pt nanoparticles for oxygen reduction reaction in direct methanol fuel cells.[5] However, AuPt alloy nanoparticles are metastable and difficult to synthesize due to their miscibility gap,[6−9] and a great deal of efforts have been devoted to kinetically trap AuPt alloy nanoparticles, usually via simultaneous reduction of the respective metal salt precursors in the presence of surfactants and reducing agents at elevated temperatures, which is rather complicated and often leads to gradient alloy (core−shell-like) or phase separated structures.[6−9]

A common issue in the application of nanoparticles as a catalyst is their stability, as the nanoparticles tend to aggregate, leading to gradual reduction in catalytic activity.[10] In addition, isolation and recycling of the nanoparticle catalyst after each use may be very difficult.[10] An effective strategy to prevent aggregation and facilitate handling of the metallic nanoparticles is to immobilize the nanoparticles on supports such as inorganic materials,[4,11,12] carbon materials,[13,14] and various polymer matrices.[10,15−18] Polyelectrolyte multilayers (PEMs), which can be facilely fabricated via the layer-by-layer technique on a variety of substrates of different shapes and sizes with well-controlled composition and thickness,[19] have been employed as versatile nanoreactors for the synthesis of various monometallic nanoparticles as well as Au−Ag alloy and core−shell nanoparticles.[20−25]

In this report we show that metastable AuPt alloy nanoparticles of different compositions can be conveniently synthesized by coreduction of chloroaurate and chloroplatinate ions *in situ* in a polymer matrix. The PEM-supported alloy nanoparticles exhibited superior catalytic activity for the reduction of 4-nitrophenol as compared to monometallic Au or Pt nanoparticles, and the catalytic activity of the nanoparticles depended on the alloy composition.

EXPERIMENTAL SECTION

Materials. Hexachloroplatinum(IV) acid hydrate ($H_2PtCl_6·6H_2O$) was purchased from Shanghai First Reagent Factory. Chloroauric acid tetrahydrate ($HAuCl_4·4H_2O$) was obtained from Sinopharm Chemical Reagent Co., Ltd. Sodium chloride (NaCl), hydrogen peroxide, sodium borohydride ($NaBH_4$), sulfuric acid (H_2SO_4), and 4-nitrophenol, all of analytical grade, were purchased from Beijing Chemical Reagents Company. Poly(diallyldimethylammonium chloride) (PDDA, 20 wt % in water, Mw ≈ 200−350k) and poly(styrenesulfonate) (PSS, Mw ≈ 70k) were obtained from Aldrich. All chemicals were used as received without further purification. Freshly prepared ultrapure water (Millipore Milli-Q, 18.2 MΩ cm at 25 °C) was used in all experiments.

Preparation of $(PDDA/PSS)_{4.5}$ Film. Quartz slides (1 cm × 3 cm) and glass slides (2 cm × 2 cm) were cleaned in a boiling piranha solution (98% H_2SO_4:30% H_2O_2, 70:30 v/v) at 80 °C for 1 h and then

Received: October 23, 2014
Revised: November 29, 2014

   dx.doi.org/10.1021/la5042019 | Langmuir XXXX, XXX, XXX−XXX

washed by copious amounts of water. A freshly cleaned slide was immersed sequentially into PDDA (1.0 mg/mL) and PSS (1.0 mg/mL) aqueous solutions containing 1.5 M concentration of NaCl for 30 min each, with sufficient water rinsing in between, and the process was repeated until 4.5 bilayers were deposited on the substrate, producing a PEM capped by PDDA (or PEM for short). The thickness of the PEM was about 30 nm.

Synthesis of PEM-Supported Au–Pt Alloy Nanoparticles. Mixture solutions of $HAuCl_4$ and H_2PtCl_6 with a total concentration of 1 mM and different $HAuCl_4/H_2PtCl_6$ ratios were prepared. A $(PDDA/PSS)_{4.5}$ PEM film was dipped into a mixture solution for 5 min, removed, and rinsed with water, and then treated with a freshly prepared aqueous solution of $NaBH_4$ (0.10 M) for 5 min to reduce the precursor ions in the film to produce metal nanoparticles.

Characterization. UV–vis spectra of the PEM containing the precursor ions or the nanoparticles were collected on a TU1901 spectrometer (Beijing Purkinje General Instrument Co., Ltd.) at room temperature. Molar ratio between the $AuCl_4^-$ and $PtCl_6^{2-}$ precursor ions in the PEM was determined from the UV–vis spectrum using a chemometrics method described in detail in the Supporting Information. Au and Pt contents in the PEMs were measured by inductively coupled plasma mass spectrometry (ICP-MS, X Series 2, Thermo Scientific). Transmission electron microscopy (TEM) and selected-area electron diffraction (SAED) characterization were carried out on a JEOL-1011 microscope operating at 100 kV accelerating voltage. A small piece of the PEM film loaded with metal nanoparticles was peeled off from the substrate using dilute hydrofluoric acid, floated in water, and then transferred to a carbon-coated copper grid for TEM characterization.

RESULTS AND DISCUSSION

Our strategy is schematically illustrated in Scheme 1. A PEM is assembled from two typical strong polyelectrolytes, poly-

Scheme 1. Schematic Illustration of the in Situ Synthesis of AuPt Alloy Nanoparticles in the PEM and the Synergistic Effects between Au and Pt

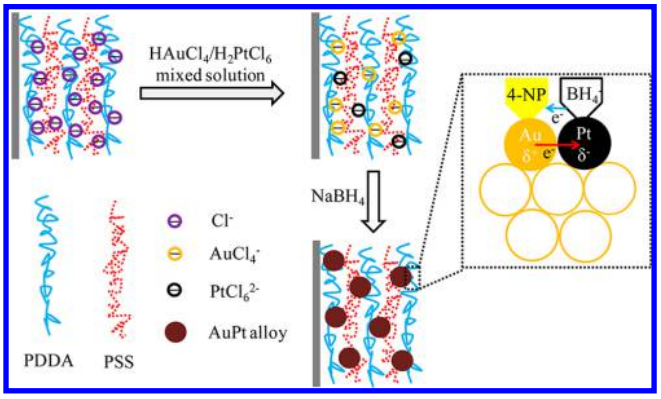

(styrenesulfonate) (PSS) and poly(diallyldimethylammonium chloride) (PDDA), with PDDA as the capping layer. The PEM is immersed into a mixture solution of chloroauric and chloroplatinic acids to exchange the Cl^- counterions present in the as-assembled PEM for $AuCl_4^-$ and $PtCl_6^{2-}$ ions,[22,25] removed and rinsed with water, and then treated with $NaBH_4$ to produce AuPt alloy nanoparticles in the PEM. The ion exchange between the PEM and the solution is rapid,[26] and the time we used (5 min) was sufficient for the exchange to reach equilibrium. Figure 1a presents the UV–vis spectra of the PEMs immersed into $HAuCl_4/H_2PtCl_6$ mixture solutions of different composition ratios. For the PEM treated with $HAuCl_4$ solution, two strong peaks emerged at ~230 and ~325 nm, respectively, characteristic of the $AuCl_4^-$ ion,[27] whereas the PEM dipped into the H_2PtCl_6 solution exhibited two different peaks at ~208 and ~270 nm, characteristic of the $PtCl_6^{2-}$ ion.[28] These four peaks were observed in the UV–vis spectra of the PEMs ion-exchanged with the mixture solutions, clearly indicating that both $AuCl_4^-$ and $PtCl_6^{2-}$ ions were incorporated into the PEMs. Due to significant overlaps between the peaks, the contents of the two ions in the PEMs were quantified from the UV–vis spectra using a chemometrics method (Supporting Information). Figure 1b plots the mole fraction of $AuCl_4^-$ ion in the PEM as a function of that in the mixture solution. It can be seen that the curve deviates from a linear relationship, with a higher $AuCl_4^-$ content in the PEM than in the corresponding solution, indicating that the association of the PDDA ammonium unit with the $AuCl_4^-$ ion is slightly more favorable than with the $PtCl_6^{2-}$ ion. The metal precursor ions in the PEM were readily reduced into metal nanoparticles *in situ* using $NaBH_4$ (0.1 M) as a reducing agent.[22,25] The Au and Pt contents in the PEMs were analyzed by ICP-MS, and the results are also presented in Figure 1b, which are in excellent agreement with that of the precursor ion contents in the PEM, indicating complete reduction of both ions and the validity of the chemometrics method. The plots show that the contents of the metals in the PEM can be conveniently controlled by varying the concentration ratio of the mixture solution. Hereafter the metal nanoparticles are denoted Au_xPt_{100-x}, where x is the mole percentage of Au in the AuPt nanoparticles.

Next we examined the structure of the bimetallic nanoparticles. There are three possible structures for bimetallic nanoparticles, namely core–shell, mixture, and alloy.[1,6] Figure 2a displays the UV–vis spectra of the various AuPt nanoparticles synthesized in the PEM. Au nanoparticles are known to exhibit a strong surface plasmon resonance (SPR) peak in the visible region. This peak was observed at ~530 nm in the spectrum of the PEM containing Au nanoparticles, as expected. The Au SPR peak, however, was absent in the spectra of all other PEMs, even the one loaded with $Au_{86}Pt_{14}$ nanoparticles (Figure 2a). This phenomenon is distinct from that of physical mixtures of Au and Pt nanoparticles, since the mixture always displays the Au SPR peak, the peak intensity depending on the content of Au. Core–shell structure nanoparticles, either Pt@Au or Au@Pt, also exhibit the Au SPR peak, although for the latter the peak intensity decreases with increasing thickness of the Pt shell.[29,30] Therefore, the UV–vis data rule out the core–shells (either Au@Pt or Pt@Au) and mixture structures, and suggest that the AuPt nanoparticles were alloys. The nanoparticles were further characterized by selected area electron diffraction (SAED), and the lattice parameter of the AuPt nanoparticles obtained from the (111) diffraction as a function of the Au content is depicted in Figure 2b. A linear relationship between the lattice parameter and the composition is observed, in accordance with Vegard's law,[31] further confirming the formation of AuPt alloy nanoparticles. It should be pointed out that similar coreduction of Au and Pt precursors by $NaBH_4$ in aqueous solution produced phase-separated structures, and a strong reducing agent such as hot butyllithium was required to rapidly reduce the precursors and kinetically trap the alloy structures.[6] The comparison signifies the important role the PEM plays in the process as a nanoreactor. Both $AuCl_4^-$ and $PtCl_6^{2-}$ precursor ions are homogeneously distributed in the PEM, and the mobility of the ions as well as the metal atoms and clusters produced from their reduction is greatly hindered by the polymer matrix, so that phase separation is suppressed, resulting in formation of alloy nanoparticles under the mild

dx.doi.org/10.1021/la5042019 | Langmuir XXXX, XXX, XXX–XXX

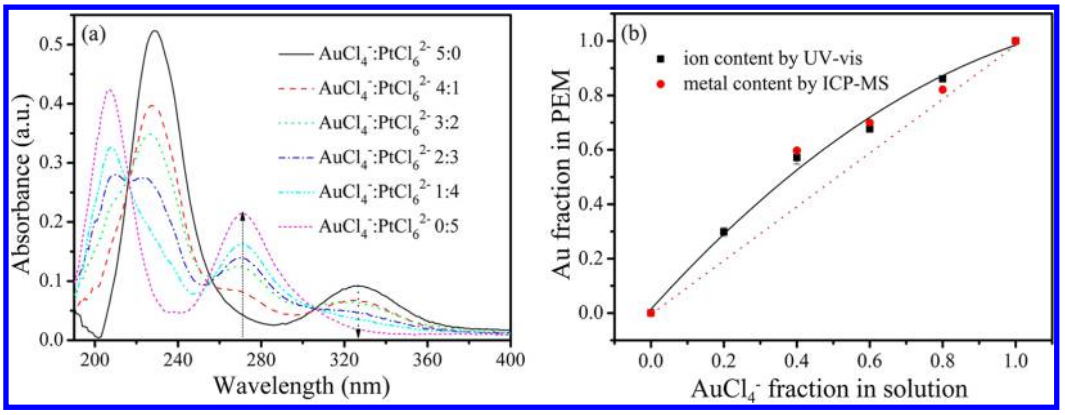

Figure 1. (a) UV−vis spectra of the precursor ions exchanged into PEMs from mixture solution of different $HAuCl_4$-to-H_2PtCl_6 ratios. (b) Mole fractions of Au precursor ions (black squares) and metallic Au after in situ reduction (red circles) as functions of mole fraction of $AuCl_4^-$ in the solution.

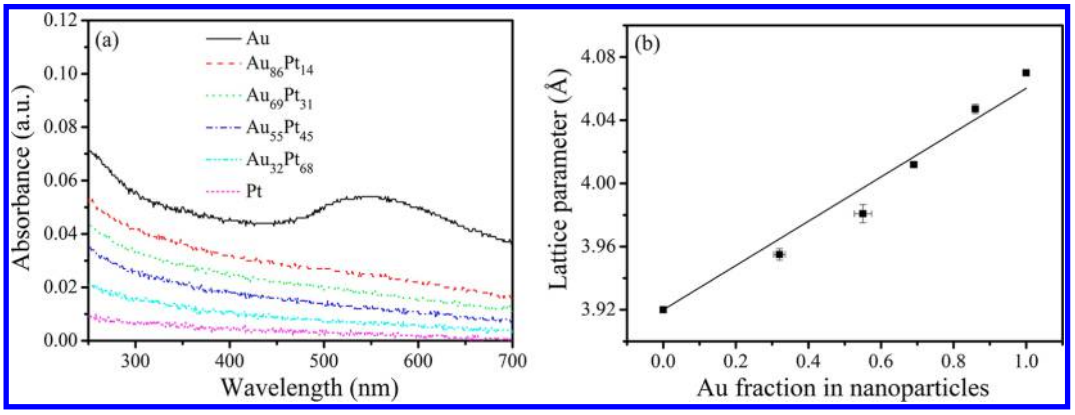

Figure 2. (a) UV−vis spectra of AuPt nanoparticles of different compositions. (b) Lattice parameter for the nanoparticles as a function of the mole fraction of Au.

conditions. In a separate controlled experiment, $NaBH_4$ solutions of different concentrations were used to reduce the precursor ions in the PEM. As seen in the UV−vis spectra presented in Figure 3, while the Au SPR band is absent at a $NaBH_4$ concentration of 100 mM, as discussed above, it starts to emerge at 10 mM, and is much stronger at 1 mM $NaBH_4$ concentration, which indicates that heterostructured nanoparticles were also generated in the PEM in the latter two cases. At low $NaBH_4$ concentrations, the reduction of the precursor ions is slower, and apparently phase separation is allowed under these conditions.

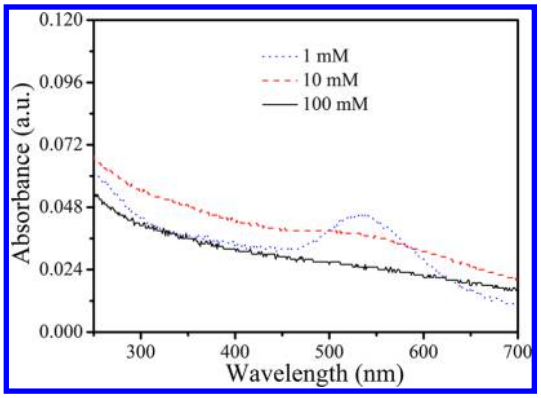

Figure 3. UV−vis spectra of the AuPt bimetallic nanoparticles in the PEM generated via reduction of the precursor ions with $NaBH_4$ of different concentrations.

Figure 4 shows TEM images and particle size distributions of the metallic nanoparticles in the PEMs. Obviously, the spherical nanoparticles (Figure S5, Supporting Information) with a narrow size distribution were well-dispersed in the polymer matrices. The particle size increased with the Au content, consistent with previous reports.[4,7] This is because the $AuCl_4^-$ ion is monovalent and $PtCl_6^{2-}$ ion is divalent, and a same PEM can bind twice the amount of $AuCl_4^-$ as that of $PtCl_6^{2-}$ via ion exchange, and subsequently more metallic Au and Pt are produced in the PEM at a higher Au/Pt ratio.

Finally, we examined the catalytic activity of these PEM-supported AuPt alloy nanoparticles. Catalytic reduction of 4-nitrophenol into 4-aminophenol is an important reaction in pharmaceutical and fine chemicals industries,[32] and use of various metallic nanoparticles, including Ag,[13,17] Au,[33] Au@Ag,[25] Cu,[34] Pd,[17] Pt,[17,35] as catalyst in this reaction has been explored. This reaction can be conveniently tracked by UV−vis absorption spectroscopy. After addition of $NaBH_4$ as the reducing agent into 4-nitrophenol aqueous solution, a strong absorption peak emerged in the UV−vis spectrum at 400 nm, due to the formation of 4-nitrophenolate anions under basic conditions (Figure 5).[36] Without the metallic nanoparticles as the catalyst, the reduction reaction does not proceed.[25] When a nanoparticles-containing PEM on a quartz substrate was introduced into the mixed solution, the intensity of this peak gradually decreased as the reaction progressed with time

dx.doi.org/10.1021/la5042019 | Langmuir XXXX, XXX, XXX−XXX

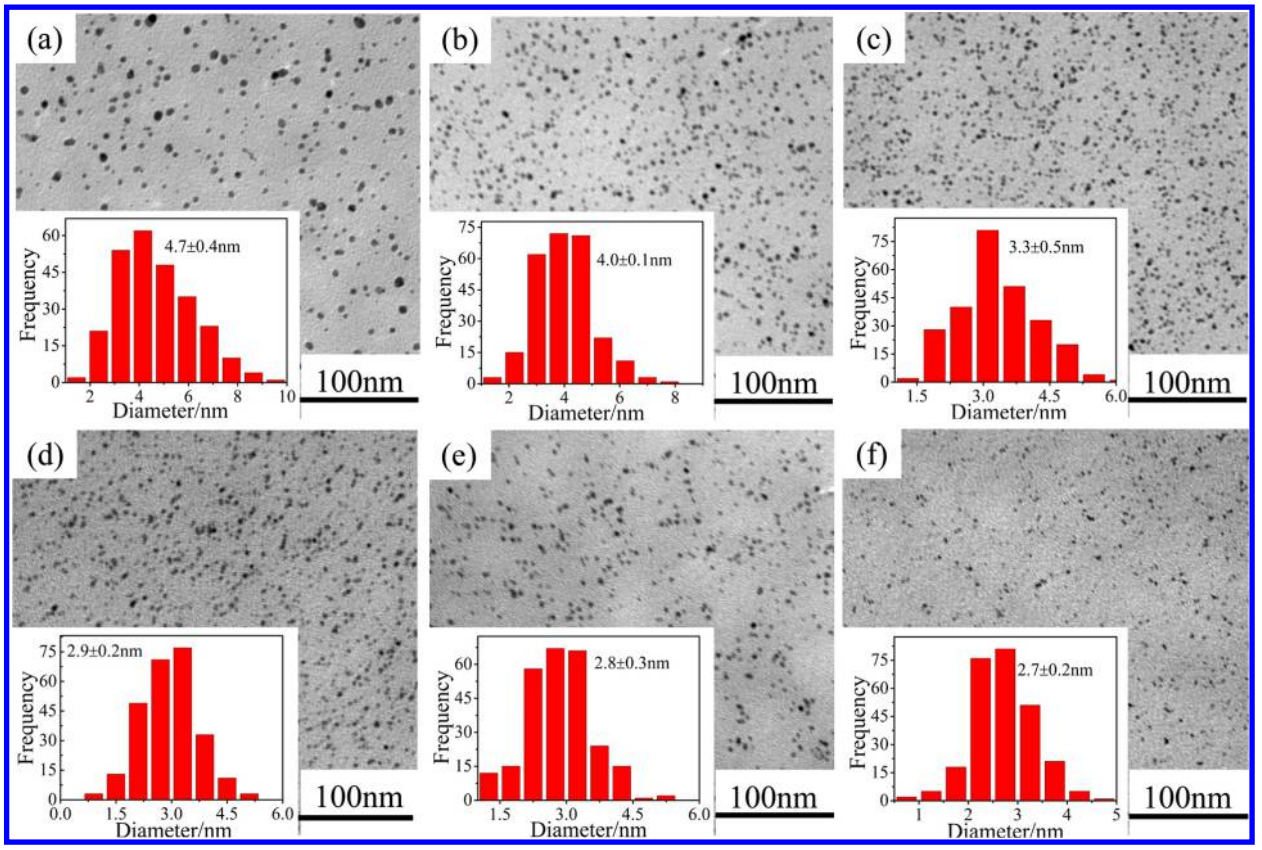

Figure 4. TEM images and corresponding size distribution histograms of the nanoparticles: (a) Au, (b) $Au_{86}Pt_{14}$, (c) $Au_{69}Pt_{31}$, (d) $Au_{55}Pt_{45}$, (e) $Au_{32}Pt_{68}$, and (f) Pt.

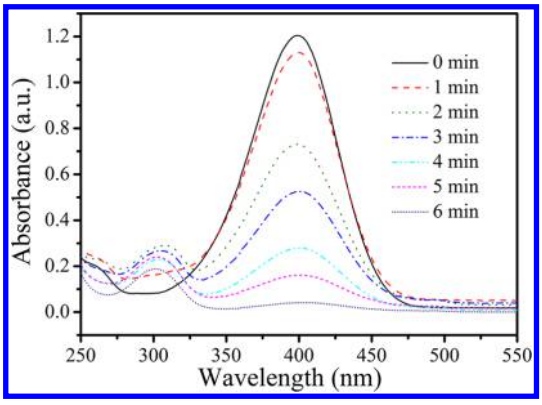

Figure 5. Time-dependent UV−vis absorption spectra showing the reduction of 4-nitrophenol by $NaBH_4$ in the presence of PEM-supported $Au_{55}Pt_{45}$ alloy nanoparticles.

(Figure 5). It has been reported that an induction period exists for this reaction.[37−42] In our study, we observed early on this induction period as well when the water for making the solutions was stored for some time prior to use, but once we used freshly prepared water in the experiments, the induction period completely disappeared. This finding suggests that O_2 dissolved in the water was responsible for the induction period, consistent with earlier reports.[39,40] In order to avoid possible interference by this issue, fresh water was used in all our experiments. Figure 6a displays as a function of time the absorption intensity of the peak at 400 nm, which represents the concentration of 4-nitrophenolate ion. Linear correlation is observed in all cases. This is because both $NaBH_4$ and 4-nitrophenol were in large excess as compared to the amount of the catalyst, and the reaction can be considered pseudo-zero-order, which is well-known in heterogeneous catalysis.[43] The slope of the straight line is the apparent rate constant k_{app} for the reaction. To better compare the activity among different catalysts in heterogeneous catalysis, the rate constant should be normalized against the total surface area of the catalyst.[44] Figure 6b plots the normalized apparent rate constant k_{app} as a function of the nanoparticle composition. A "volcano-shape" relationship is observed with a maximum activity at a Au/Pt ratio of about 2:1, which clearly indicates synergistic effects between Au and Pt in the catalysis.

It is well-established that, in the reduction of 4-nitrophenol by $NaBH_4$, electron transfer from BH_4^- to 4-nitrophenol takes place only when both species are absorbed on the surface of the catalyst,[14,15,40] and it was found that 4-nitrophenol prefers to adsorb on Au, whereas BH_4^- is more likely to adsorb on Pt.[41] Previous work also indicates that excess electrons on Au atoms can transfer to the adjacent Pt atoms in a AuPt alloy.[4] On the basis of the above, we propose the following mechanism of synergistic catalysis between Au and Pt, as depicted in Scheme 1: (1) 4-nitrophenolate and BH_4^- adsorb to neighboring Au and Pt atoms, respectively, at the surface of a AuPt alloy nanoparticle; (2) Au atoms transfer their excess electrons to the adjacent Pt atoms, resulting in electron enrichment onto the Pt atoms, which in turn facilitates the electron transfer[45] from the adsorbed BH_4^- to the 4-nitrophenolate adsorbed nearby on the Au.

dx.doi.org/10.1021/la5042019 | *Langmuir* XXXX, XXX, XXX−XXX

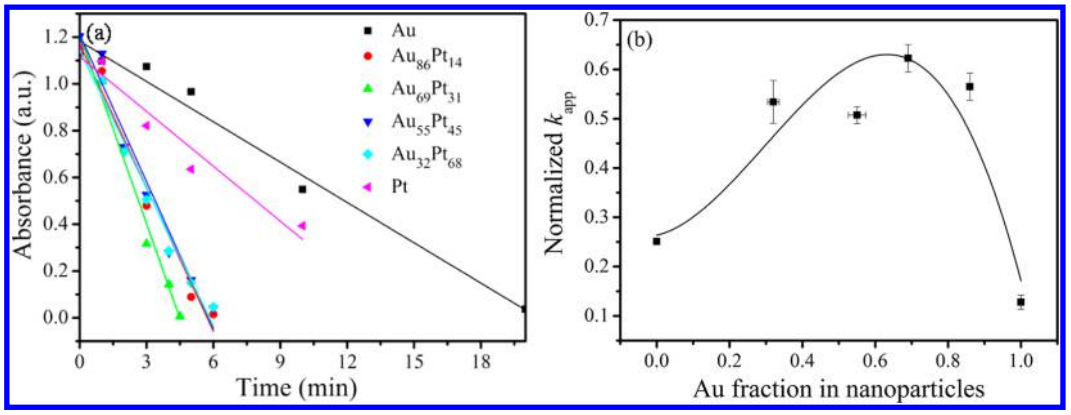

Figure 6. (a) UV absorption intensity at 400 nm as a function of time for the reduction of 4-nitrophenol catalyzed by different PEM-supported nanoparticles. (b) Dependence of the apparent rate constant k_{app} normalized to total surface area of the nanoparticles on the mole fraction of Au in the nanoparticles.

CONCLUSION

We have presented a facile strategy for *in situ* synthesis of metastable AuPt alloy nanoparticles in polymer supports, in which the PEM matrix helps suppress the Au−Pt phase separation and enables alloy nanoparticle formation in a wide composition range under mild conditions. The PEM-supported AuPt alloy nanoparticles were found to be superior in catalytic performance to the corresponding monometallic ones due to synergistic effects between neighboring Au and Pt atoms in the alloys. This work provides a simple route to synthesis of polymer-supported alloy nanoparticles, which may find application as catalysts in various industrial processes.

ASSOCIATED CONTENT

Supporting Information

Determination of the ion contents in the PEM, SAED, and additional TEM and UV data. This material is available free of charge via the Internet at http://pubs.acs.org.

AUTHOR INFORMATION

Corresponding Author

*Phone: (+86)431-85262854. Fax: (+86)431-85262126. E-mail: zhsu@ciac.ac.cn.

Notes

The authors declare no competing financial interest.

ACKNOWLEDGMENTS

Financial support from the National Natural Science Foundation of China (21174145) is gratefully acknowledged.

REFERENCES

(1) Wang, D. S.; Li, Y. D. Bimetallic Nanocrystals: Liquid-Phase Synthesis and Catalytic Applications. *Adv. Mater.* **2011**, *23*, 1044−1066.

(2) Nam, J. M.; Stoeva, S. I.; Mirkin, C. A. Bio-Bar-Code-Based DNA Detection with PCR-like Sensitivity. *J. Am. Chem. Soc.* **2004**, *126*, 5932−5933.

(3) Liu, Y. C.; Yu, C. C.; Hsu, T. C. Trace Molecules Detectable by Surface-Enhanced Raman Scattering Based on Newly Developed Ag and Au Nanoparticles-Containing Substrates. *Electrochem. Commun.* **2007**, *9*, 639−644.

(4) Tongsakul, D.; Nishimura, S.; Ebitani, K. Platinum/Gold Alloy Nanoparticles-Supported Hydrotalcite Catalyst for Selective Aerobic Oxidation of Polyols in Base-Free Aqueous Solution at Room Temperature. *ACS Catal.* **2013**, *3*, 2199−2207.

(5) Selvarani, G.; Selvaganesh, S. V.; Krishnamurthy, S.; Kiruthika, G. V. M; Sridhar, P.; Pitchumani, S.; Shukla, A. K. A Methanol-Tolerant Carbon-Supported Pt-Au Alloy Cathode Catalyst for Direct Methanol Fuel Cells and Its Evaluation by DFT. *J. Phys. Chem. C* **2009**, *113*, 7461−7468.

(6) Zhou, S. H.; Jackson, G. S.; Eichhorn, B. AuPt Alloy Nanoparticles for CO-Tolerant Hydrogen Activation: Architectural Effects in Au-Pt Bimetallic Nanocatalysts. *Adv. Funct. Mater.* **2007**, *17*, 3099−3104.

(7) Wu, M. L.; Chen, D. H.; Huang, T. C. Preparation of Au/Pt Bimetallic Nanoparticles in Water-in-Oil Microemulsions. *Chem. Mater.* **2001**, *13*, 599−606.

(8) Wanjala, B. N.; Luo, J.; Loukrakpam, R.; Fang, B.; Mott, D.; Njoki, P. N.; Engelhard, M.; Naslund, H. R.; Wu, J. K.; Wang, L. C.; Malis, O.; Zhong, C. J. Nanoscale Alloying, Phase-Segregation, and Core-Shell Evolution of Gold-Platinum Nanoparticles and Their Electrocatalytic Effect on Oxygen Reduction Reaction. *Chem. Mater.* **2010**, *22*, 4282−4294.

(9) Njoki, P. N.; Luo, J.; Wang, L. Y.; Maye, M. M.; Quaizar, H.; Zhong, C. J. Platinum-Catalyzed Synthesis of Water-Soluble Gold-Platinum Nanoparticles. *Langmuir* **2005**, *21*, 1623−1628.

(10) Schrinner, M.; Proch, S.; Mei, Y.; Kempe, R.; Miyajima, N.; Ballauff, M. Stable Bimetallic Gold-Platinum Nanoparticles Immobilized on Spherical Polyelectrolyte Brushes: Synthesis, Characterization, and Application for the Oxidation of Alcohols. *Adv. Mater.* **2008**, *20*, 1928−1933.

(11) Abad, A.; Corma, A.; García, H. Catalyst Parameters Determining Activity and Selectivity of Supported Gold Nanoparticles for the Aerobic Oxidation of Alcohols: The Molecular Reaction Mechanism. *Chem.—Eur. J.* **2008**, *14*, 212−222.

(12) Mori, K.; Hara, T.; Mizugaki, T.; Ebitani, K.; Kaneda, K. Hydroxyapatite-Supported Palladium Nanoclusters: A Highly Active Heterogeneous Catalyst for Selective Oxidation of Alcohols by Use of Molecular Oxygen. *J. Am. Chem. Soc.* **2004**, *126*, 10657−10666.

(13) Zhang, P.; Shao, C. L.; Zhang, Z. Y.; Zhang, M. Y.; Mu, J. B.; Guo, Z. C.; Liu, Y. C. In Situ Assembly of Well-Dispersed Ag Nanoparticles (AgNPs) on Electrospun Carbon Nanofibers (CNFs) for Catalytic Reduction of 4-Nitrophenol. *Nanoscale* **2011**, *3*, 3357−3363.

(14) Tang, S. C.; Vongehr, S.; Meng, X. K. Controllable Incorporation of Ag and Ag-Au Nanoparticles in Carbon Spheres for Tunable Optical and Catalytic Properties. *J. Mater. Chem.* **2010**, *20*, 5436−5445.

(15) Lu, Y.; Yuan, J. Y.; Polzer, F.; Drechsler, M.; Preussner, J. In Situ Growth of Catalytic Active AuPt Bimetallic Nanorods in Thermoresponsive Core-Shell Microgels. *ACS Nano* **2010**, *4*, 7078−7086.

(16) Liu, J. Y.; Cheng, L.; Song, Y. H.; Liu, B. F.; Dong, S. J. Simple Preparation Method of Multilayer Polymer Films Containing Pd Nanoparticles. *Langmuir* **2001**, *17*, 6747−6750.

(17) Esumi, K.; Isono, R.; Yoshimura, T. Preparation of PAMAM- and PPI-Metal(Silver, Platinum, and Palladium) Nanocomposites and Their Catalytic Activities for Reduction of 4-Nitrophenol. *Langmuir* **2004**, *20*, 237−243.
(18) Kidambi, S.; Dai, J. H.; Li, J.; Bruening, M. L. Selective Hydrogenation by Pd Nanoparticles Embedded in Polyelectrolyte Multilayers. *J. Am. Chem. Soc.* **2004**, *126*, 2658−2659.
(19) Decher, G. Fuzzy Nanoassemblies: Toward Layered Polymeric Multicomposites. *Science* **1997**, *277*, 1232−1237.
(20) Joly, S.; Kane, R.; Radzilowski, L.; Wang, T.; Wu, A.; Cohen, R. E.; Thomas, E. L.; Rubner, M. F. Multilayer Nanoreactors for Metallic and Semiconducting Particles. *Langmuir* **2000**, *16*, 1354−1359.
(21) Dai, J. H.; Bruening, M. L. Catalytic Nanoparticles Formed by Reduction of Metal Ions in Multilayered Polyelectrolyte Films. *Nano Lett.* **2002**, *2*, 497−501.
(22) Zhang, X.; Zan, X. J.; Su, Z. H. Polyelectrolyte Multilayer Supported Pt Nanoparticles as Catalysts for Methanol Oxidation. *J. Mater. Chem.* **2011**, *21*, 17783−17789.
(23) Kidambi, S.; Bruening, M. L. Multilayered Polyelectrolyte Films Containing Palladium Nanoparticles: Synthesis, Characterization, and Application in Selective Hydrogenation. *Chem. Mater.* **2005**, *17*, 301−307.
(24) Shang, L.; Jin, L. H.; Guo, S. J.; Zhai, J. F.; Dong, S. J. A Facile and Controllable Strategy to Synthesize Au-Ag Alloy Nanoparticles within Polyelectrolyte Multilayer Nanoreactors upon Thermal Reduction. *Langmuir* **2010**, *26*, 6713−6719.
(25) Zhang, X.; Su, Z. H. Polyelectrolyte-Multilayer-Supported Au@Ag Core-Shell Nanoparticles with High Catalytic Activity. *Adv. Mater.* **2012**, *24*, 4574−4577.
(26) Wang, L. M.; Lin, Y.; Peng, B.; Su, Z. H. Tunable Wettability by Counterion Exchange at the Surface of Electrostatic Self-Assembled Multilayers. *Chem. Commun.* **2008**, 5972−5974.
(27) Goi, D. V.; Matijević, E. Tailoring the Particle Size of Monodispersed Colloidal Gold. *Colloids Surf., A* **1999**, *146*, 139−152.
(28) Castro, E. G.; Salvatierra, R. V.; Schreiner, W. H.; Oliveira, M. M.; Zarbin, A. J. G. Dodecanethiol-Stabilized Platinum Nanoparticles Obtained by a Two-Phase Method: Synthesis, Characterization, Mechanism of Formation, and Electrocatalytic Properties. *Chem. Mater.* **2010**, *22*, 360−370.
(29) Luo, J.; Wang, L. Y.; Mott, D.; Njoki, P. N.; Lin, Y.; He, T.; Xu, Z. C.; Wanjana, B. N.; Lim, I. I. S.; Zhong, C. J. Core/Shell Nanoparticles as Electrocatalysts for Fuel Cell Reactions. *Adv. Mater.* **2008**, *20*, 4342−4347.
(30) Henglein, A. Preparation and Optical Aborption Spectra of $Au_{core}Pt_{shell}$ and $Pt_{core}Au_{shell}$ Colloidal Nanoparticles in Aqueous Solution. *J. Chem. Phys. B* **2000**, *104*, 2201−2203.
(31) Bond, G. C. The Electronic Structure of Platinum-Gold Alloy Particles. *Platinum Met. Rev.* **2007**, *51*, 63−68.
(32) Downing, R. S.; Kunkeler, P. J.; Bekkum, H. V. Catalytic Syntheses of Aromatic Amines. *Catal. Today* **1997**, *37*, 121−136.
(33) Dotzauer, D. M.; Dai, J. H.; Sun, L.; Bruening, M. L. Catalytic Membranes Prepared Using Layer-by-Layer Adsorption of Polyelectrolyte/Metal Nanoparticle Films in Porous Supports. *Nano Lett.* **2006**, *6*, 2268−2272.
(34) Feng, Z. V.; Lyon, J. L.; Croley, J. S.; Crooks, R. M.; Bout, D. A. V.; Stevenson, K. J. Synthesis and Catalytic Evaluation of Dendrimer-Encapsulated Cu Nanoparticles. *J. Chem. Educ.* **2009**, *86*, 368−372.
(35) Mei, Y.; Sharma, G.; Lu, Y.; Ballauff, M.; Drechsler, M.; Irrgang, T.; Kempe, R. High Catalytic Activity of Platinum Nanoparticles Immobilized on Spherical Polyelectrolyte Brushes. *Langmuir* **2005**, *21*, 12229−12234.
(36) Shin, Y.; Dohnalkova, A.; Lin, Y. H. Preparation of Homogeneous Gold-Silver Alloy Nanoparticles Using the Apoferritin Cavity As a Nanoreactor. *J. Phys. Chem. C* **2010**, *114*, 5985−5989.
(37) Zeng, J.; Zhang, Q.; Chen, J. Y.; Xia, Y. N. A Comparison Study of the Catalytic Properties of Au-Based Nanocages, Nanoboxes, and Nanoparticles. *Nano Lett.* **2010**, *10*, 30−35.
(38) Zhang, Q. F.; Blom, D. A.; Wang, H. Nanoporosity-Enhanced Catalysis on Subwavelength Au Nanoparticles: a Plasmon-Enhanced Spectroscopic Study. *Chem. Mater.* **2014**, *26*, 5131−5142.
(39) Saha, S.; Pal, A.; Kundu, S.; Basu, S.; Pal, T. Photochemical Green Synthesis of Calcium-Alginate-Stabilized Ag and Au Nanoparticles and Their Catalytic Application to 4-Nitrophenol Reduction. *Langmuir* **2010**, *26*, 2885−2893.
(40) Layek, K.; Kantam, M. L.; Shirai, M.; Nishio-Hamane, D.; Sasaki, T.; Maheswaran, H. Gold Nanoparticles Stabilized on Nanocrystalline Magnesium Oxide as an Active Catalyst for Reduction of Nitroarenes in Aqueous Medium at Room Temperature. *Green Chem.* **2012**, *14*, 3164−3174.
(41) Wunder, S.; Polzer, F.; Lu, Y.; Mei, Y.; Ballauff, M. Kinetic Analysis of Catalytic Reduction of 4-Nitrophenol by Metallic Nanoparticles Immobilized in Spherical Polyelectrolyte Brushes. *J. Phys. Chem. C* **2010**, *114*, 8814−8820.
(42) Hervés, P.; Pérez-Lorenzo, M.; Liz-Marzán, L. M.; Dzubiella, J.; Lu, Y.; Ballauff, M. Catalysis by Metallic Nanoparticles in Aqueous Solution: Model Reactions. *Chem. Soc. Rev.* **2012**, *41*, 5577−5587.
(43) Guella, G.; Patton, B.; Miotello, A. Kinetic Features of the Platinum Catalyzed Hydrolysis of Sodium Borohydride from ^{11}B NMR Measurements. *J. Phys. Chem. C* **2007**, *111*, 18744−18750.
(44) Wachs, I. E.; Phivilay, S. P.; Roberts, C. A. Reporting of Reactivity for Heterogeneous Photocatalysis. *ACS Catal.* **2013**, *3*, 2606−2611.
(45) Ghosh, S. K.; Mandal, M.; Kundu, S.; Nath, S.; Pal, T. Bimetallic Pt−Ni Nanoparticles can Catalyze Reduction of Aromatic Nitro Compounds by Sodium Borohydride in Aqueous Solution. *Appl. Catal., A* **2004**, *268*, 61−66.